

Multitransition Submillimeter CO Observations of Ultraluminous IRAS Galaxies

Dominic J. Benford (dbenford@tacos.caltech.edu)¹, Min S. Yun (msy@astro.caltech.edu)²,
Todd R. Hunter (hunter@tacos.caltech.edu)¹, Peter M. Bryant (pmb@astro.caltech.edu)²,
and Thomas G. Phillips (phillips@tacos.caltech.edu)¹

California Institute of Technology

Received _____; accepted _____

Proceedings of IAU Symposium #170, *CO: 25 Years of Millimeterwave Spectroscopy*

¹Division of Physics, Mathematics, and Astronomy, California Institute of Technology
320-47, Pasadena, CA 91125

²Division of Physics, Mathematics, and Astronomy, California Institute of Technology
105-24, Pasadena, CA 91125

ABSTRACT

We present submillimeter CO observations of 8 ultraluminous IRAS galaxies as preliminary results from a multitransition survey at the Caltech Submillimeter Observatory (CSO). To date, high signal-to-noise spectra have been obtained for all 8 galaxies in the $^{12}\text{CO } J = 2 \rightarrow 1$ and $3 \rightarrow 2$ transitions. Also, we have recently detected the CO $4 \rightarrow 3$ and $6 \rightarrow 5$ transitions in some of these objects. Observations of the higher frequency lines have been limited by the AOS backend bandwidth (500 MHz = 220 km/s at CO $6 \rightarrow 5$). As of July 1995, we have begun to extend the high frequency survey using a new AOS that covers the entire 1 GHz receiver bandwidth. We are in the process of preparing an LVG analysis of the multitransition data to better constrain the temperature and density of the molecular gas in these luminous galaxies.

1. Introduction

The molecular gas in galactic nuclei is warmer and denser than the averaged gas in galactic disks (e.g. (Hüttemeister et al. 95)). The full range of temperatures and densities present in molecular gas is best explored via a multitransition excitation analysis. It is preferable to use a bright tracer of molecular gas, such as CO, which has many observable transitions of varying excitation temperatures and densities. So far, most extragalactic observations of CO have focussed only on the $J = 1 \rightarrow 0$ transition, with an excitation temperature of 5.5 K, or on the $J = 2 \rightarrow 1$ transition, with an excitation temperature of 16.6 K. Naturally, these transitions are excited in a large portion of the molecular gas in galaxies. In order to probe the warmer, denser regions of gas, higher J transitions, with wavelengths in the submillimeter, must be observed. In the past, receiver technology was insufficient to this task. The first detections of the brightest galaxies have recently been made ((Güsten et al. 93), (Harris et al. 91)). Here we report observations of ultraluminous IRAS galaxies in higher J transitions, with correspondingly higher excitation temperatures: $J = 3 \rightarrow 2$ (33 K), $4 \rightarrow 3$ (55 K), and $6 \rightarrow 5$ (116 K).

We present some of the initial results from a recently undertaken survey to learn about the state of molecular gas in galaxies. The objects presented here are a small sample of the infrared luminous galaxies from the IRAS Bright Galaxy Sample (BGS) ((Soifer et al. 89)). They are characterized by infrared luminosities of $L_{ir} > 3 \times 10^{11} L_{\odot}$.

2. Observations and Data Reduction

2.1. Observing

The initial results presented here are the result of several nights of observing at the 10.4m CSO³ in February and May 1995. The facility SIS receivers ((Kooi et al. 94A), (Kooi et al. 95), (Kooi et al. 94B)) were used with the 1024 channel 500 MHz acousto-optical spectrometer (AOS) as the backend. Typical system temperatures in fair weather of 200 K in the CO $2 \rightarrow 1$ frequencies and 400 K in the $3 \rightarrow 2$ frequencies were obtained. Two of the galaxies were observed in periods of good weather in the CO $6 \rightarrow 5$ line with $T_{sys} \sim 3000\text{K}$, and one in the $4 \rightarrow 3$ line with $T_{sys} \sim 2000\text{K}$. The beamsizes and typical main beam efficiencies at the four frequencies are $30''$ (0.76), $20''$ (.68), $15''$ (.51), and $10''$ (.39). Careful tunings were performed to insure equal instrumental sideband ratios. In all but one case (IRAS 09111-1007 CO $2 \rightarrow 1$), the new chopping secondary was used to establish the reference position with a $60''$ throw in azimuth at a frequency of ~ 1 Hz yielding duty cycles $> 90\%$. Symmetric chop cycles were performed by switching the source between the ON and OFF beams every 10 seconds. Optical and radio pointing sessions were completed on engineering nights shortly before each observing run. Also, pointing was frequently checked on Mars, Saturn and CO point stars (depending on the time of observations) during the observations, thus we estimate our pointing accuracy to be $3''$. Observed positions were taken from CO $1 \rightarrow 0$ interferometer observations when available (e.g. (Sargent & Scoville 91); (Scoville et al. 91)).

³The Caltech Submillimeter Observatory is funded by the National Science Foundation under contract AST-9313929.

2.2. Bandwidth Synthesis

Spectra were taken using the facility 500 MHz 1024-channel acousto-optical spectrometer (AOS #3) backend (Serabyn & Chumney 91). The instantaneous bandwidth available with this spectrometer is approximately 660 km/s in the $2 \rightarrow 1$ lines and 330 km/s in the $3 \rightarrow 2$ lines. Lines from some of the galaxies fit nicely into this bandwidth at both frequencies (e.g. NGC 6090). However, the galaxies with broader lines (e.g. Arp 220) require up to 3 times the available bandwidth. With the system upgrade of the new chopping secondary in late 1994, we performed these observations as one method of determining the reliability of the spectral baselines. The problem of most of the baseline ripple that hindered extragalactic observing at the CSO in the past has been overcome by the chopping secondary. By stepping the AOS along in velocity increments (typically 50-100 km/s every ~ 5 minutes) and simply adding the spectra with no baselines applied, we obtained line shapes in all cases consistent with published lower-frequency CO $1 \rightarrow 0$ spectra from these sources. The stability of the absolute level and slope across the band allowed us to successfully apply this *bandwidth synthesis* strategy, as shown in Figure 1. The raw spectra of Mrk 273 are shown, smoothed to the resolution of later figures. Three tuning sets were used to produce three separate spectra, none of which completely encloses the line. The three spectra are overlayed to demonstrate graphically the validity of this technique.

2.3. Data Reduction

All spectra were analyzed with the CLASS software package and are presented on a Rayleigh-Jeans main beam brightness temperature (T_{mb}) scale. We estimate our calibration to be accurate within 30% and our pointing to within $3''$.

Only zero-th order baselines have been subtracted from the final summed spectra for each galaxy. First order baselines have not been applied in order to emphasize the feasibility of the observing technique. In fact, the presence of first order baselines would to some degree invalidate the technique. However, the first order component of the baseline is typically much smaller than the line peak. The spectra were corrected for the measured beam efficiencies at the time of the observation and for the relative sideband gain due to atmospheric extinction (which is usually a small factor of a few percent, especially in the $2 \rightarrow 1$ lines). The spectra displayed are Hanning smoothed to a velocity resolution ~ 5 - 10 km/s (the higher frequency $4 \rightarrow 3$ and $6 \rightarrow 5$ lines are smoothed to a greater extent).

3. Results

The spectra obtained for each galaxy are presented in Figures 2 - 11. Two Gaussian components were fit to each spectrum and their statistics are plotted on the spectra. The integrated line strengths are listed in Tables 1 and 2 below. To remove beam dilution effects, the line strengths have been convolved to a beamsize of $20''$ and re-tabulated in the next column. Finally, the line ratios are derived from the convolved line strengths. The beam-corrected flux ratio for the $3 \rightarrow 2$ to $2 \rightarrow 1$ lines is close to unity. We see that the beam-corrected fluxes decrease with increasing J above $J = 3$.

The new 1.5 GHz AOS went on-line at the CSO in early July of 1995. At that time, the program of observing these galaxies (and others) in the CO $6 \rightarrow 5$ transition began in earnest. Unfortunately, the weather was not sufficient to do much work at that frequency. However, some of the $3 \rightarrow 2$ measurements were repeated which verified that the bandwidth synthesis procedure is valid.

Of particular note is that the CSO beamsize in the CO $6 \rightarrow 5$ transition ($10''$) will match that of the IRAM 30M telescope in the $2 \rightarrow 1$ transition and should allow good

comparison of the relative line strengths.

We thank the CSO staff for their assistance during this observing project. We thank HP for providing POGs, and UChicago for providing the dropping secondary.

REFERENCES

- Güsten, R., Serabyn, E., Kasemann, C., Schinkel, A., Schneider, G., Schultz, A., & Young, K. 1993, *ApJ*, 402, 537
- Harris, A.I., Hills, R.E., Stutzki, J., Graf, U.U., Russell, A.P.G., & Genzel, R. 1991, *ApJ*, 382, L75
- Hüttemeister, S., Henkel, C., Mauersberger, R., Brouillet, N., Wiklind, T., & Millar, T.J. 1995, *A&A*, 295, 571
- Kooi, J.W., Walker, C.K., Leduc, H.G., Schaffer, P.L., Hunter, T.R., Benford, D.J., & Phillips, T.G. 1994, *Int J IR&MM Waves*, 15, 477
- Kooi, J.W., Chan, M., Bumble, B., LeDuc, H.G., & Phillips, T.G. in preparation
- Kooi, J.W., Chan, M., Bumble, B., LeDuc, H.G., Schaffer, P.L., & Phillips, T.G. 1994, *Int J IR&MM Waves*, 15, 783
- Sargent, A. & Scoville, N. 1991, *ApJ*, 366, L1
- Scoville, N.Z., Sargent, A.I., Sanders, D.B., Soifer, B.T. 1991, *ApJ*, 366, L5
- Serabyn, E., & Chumney, D. 1991, *Int J IR&MM Waves*, 12, 1493
- Soifer, B.T., Boehmer, L., Neugebauer, G., & Sanders, D.B. 1989, *AJ*, 98, 766
- Wang, Z., Scoville, N.Z., & Sanders, D.B. 1991, *ApJ*, 368, 112

Fig. 1.— An example of bandwidth synthesis observations of Mrk 273. There are three subspectra here: the central one is in dashed lines, while the two outer subspectra are in solid lines.

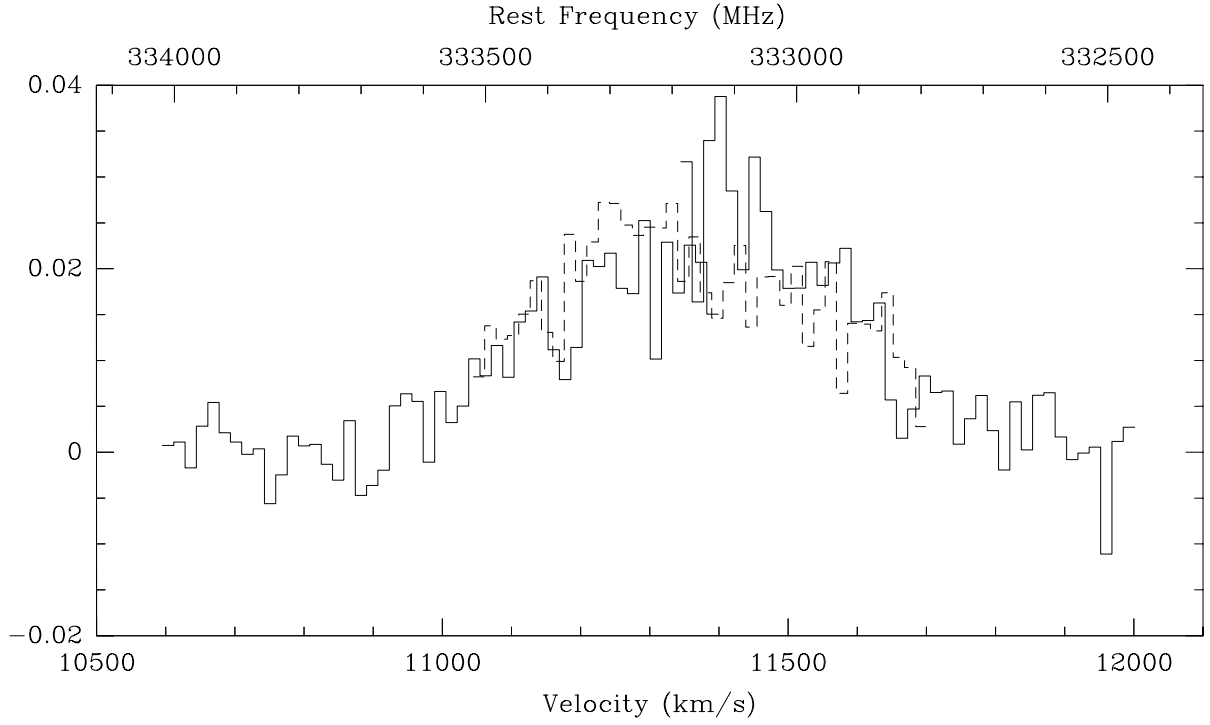


Fig. 2.— IRAS 09111-1007 in CO $3 \rightarrow 2$ and $2 \rightarrow 1$.

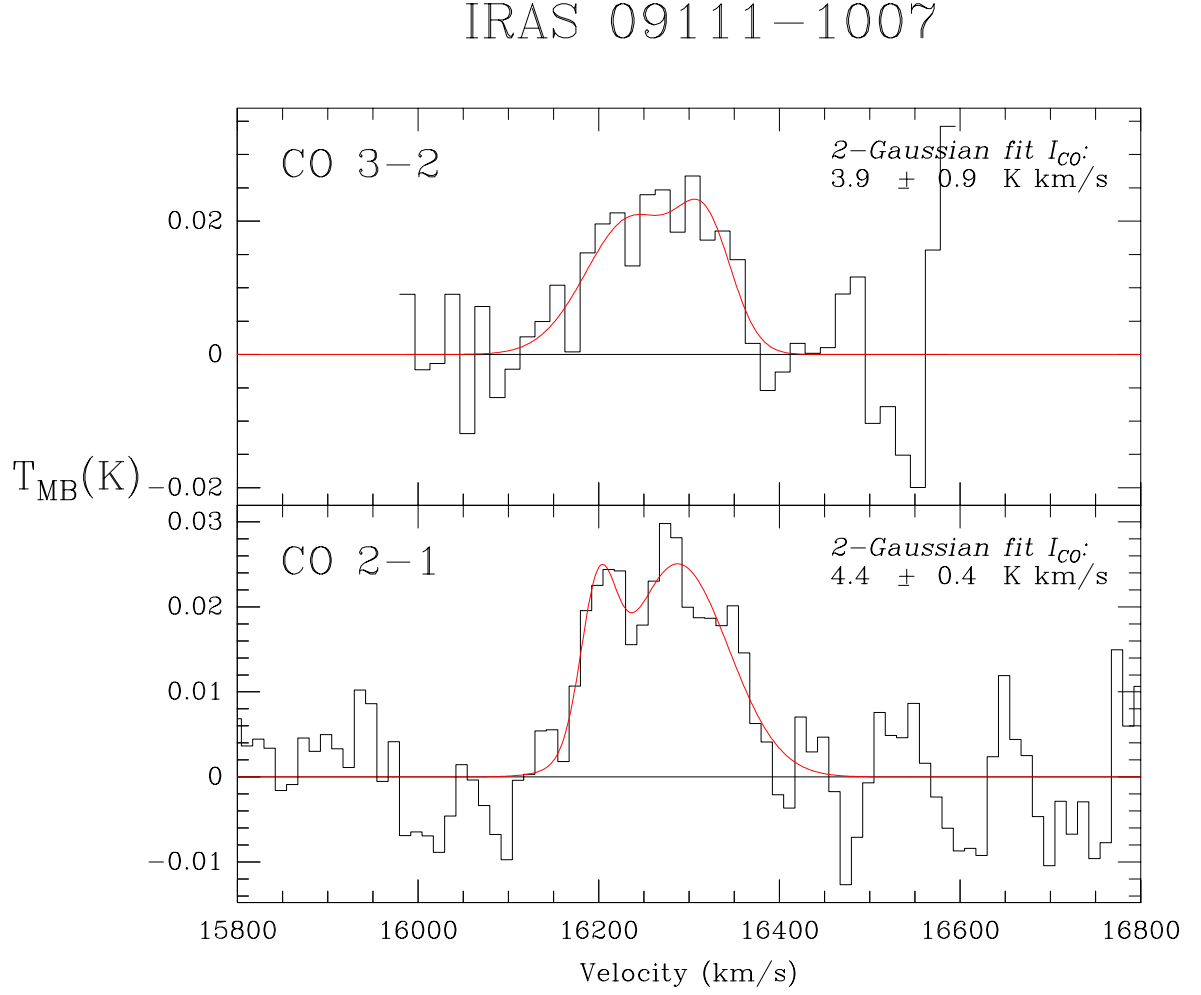


Fig. 3.— NGC 3690 in CO $3 \rightarrow 2$ and $2 \rightarrow 1$.

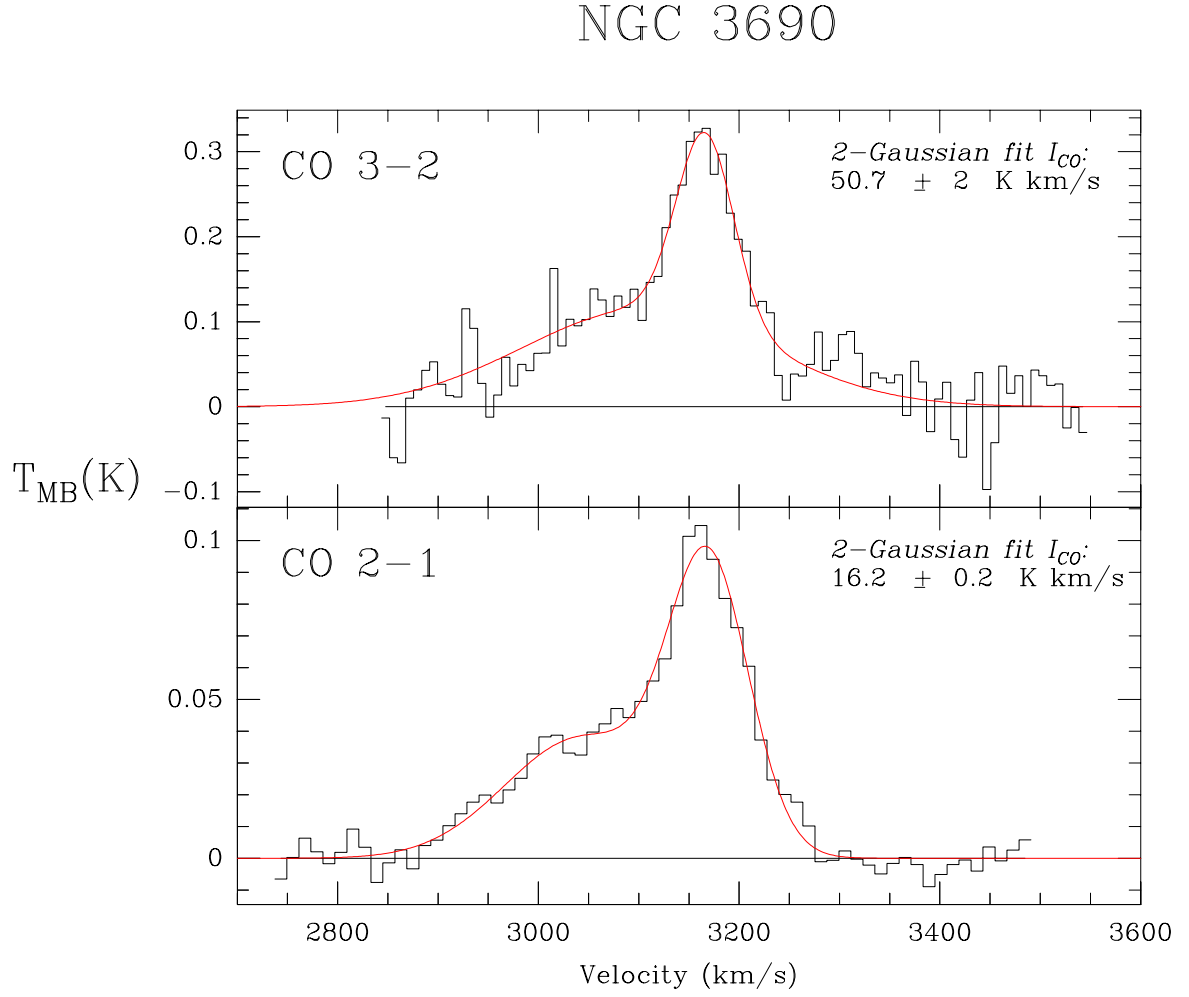


Fig. 4.— NGC 3690 in CO $6 \rightarrow 5$ and $4 \rightarrow 3$.

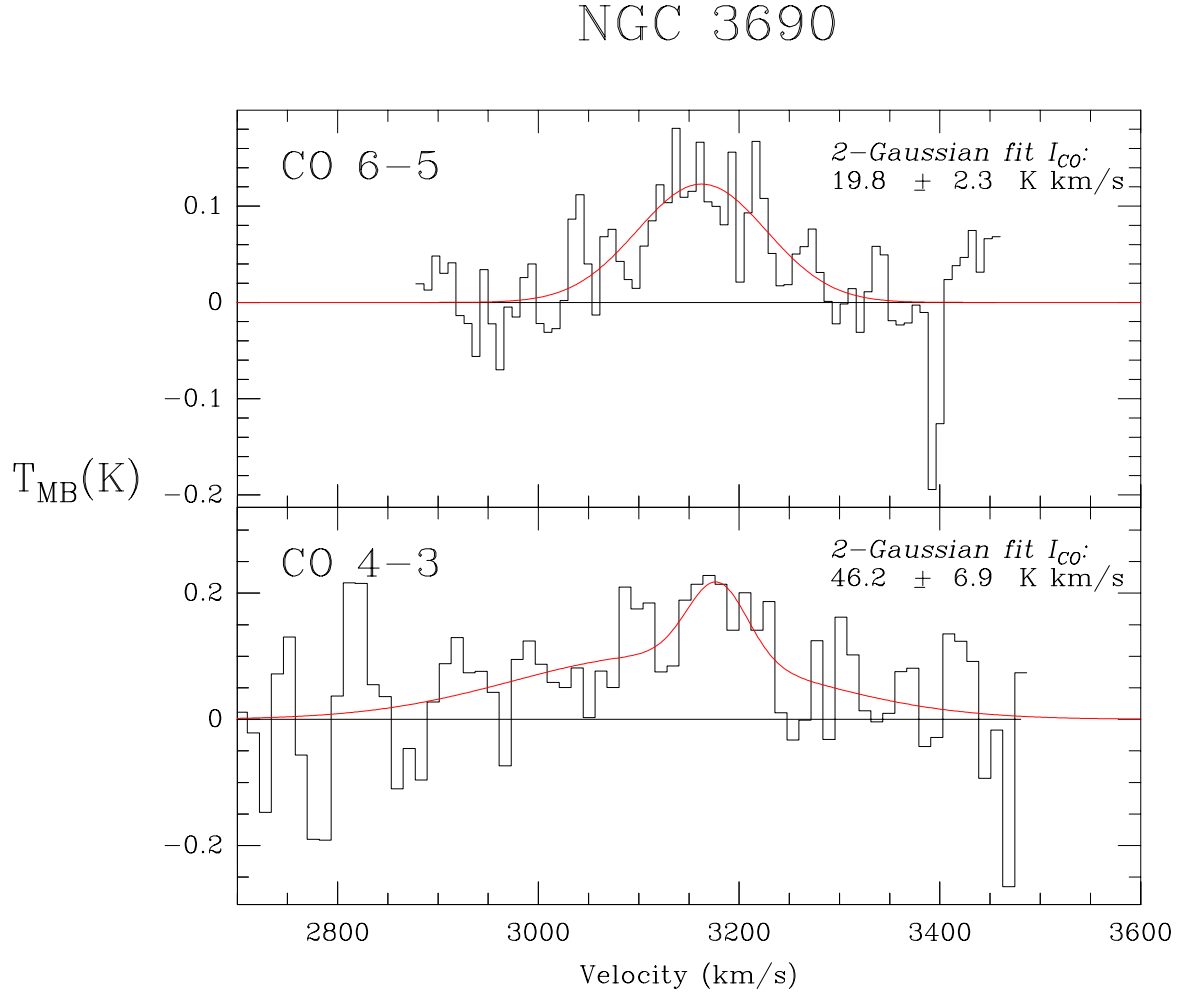


Fig. 5.— Arp 299A in CO $3 \rightarrow 2$ and $2 \rightarrow 1$. The difference in lineshapes may be due to material in the $2 \rightarrow 1$ beam but not in the $3 \rightarrow 2$ beam.

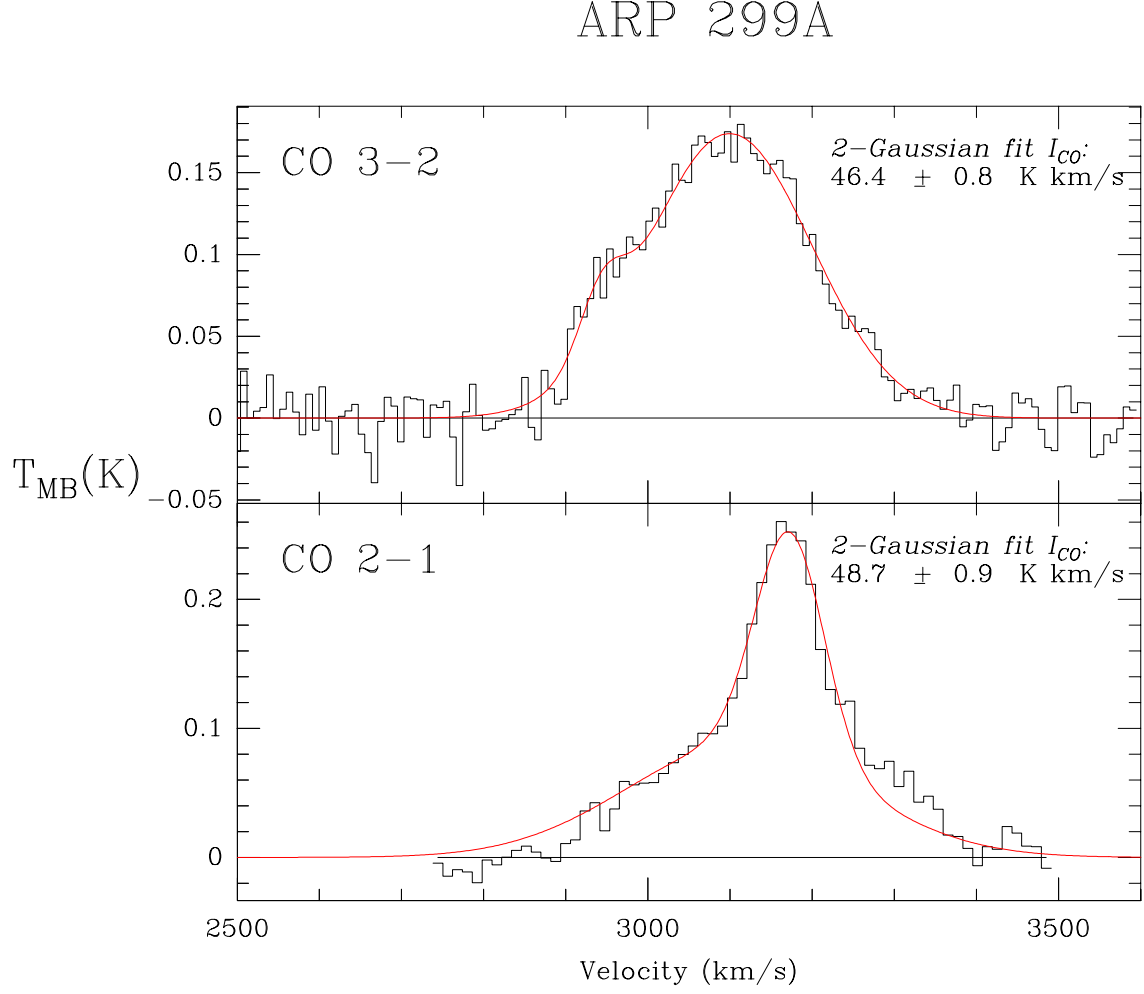


Fig. 6.— Mrk 231 in CO $3 \rightarrow 2$ and $2 \rightarrow 1$.

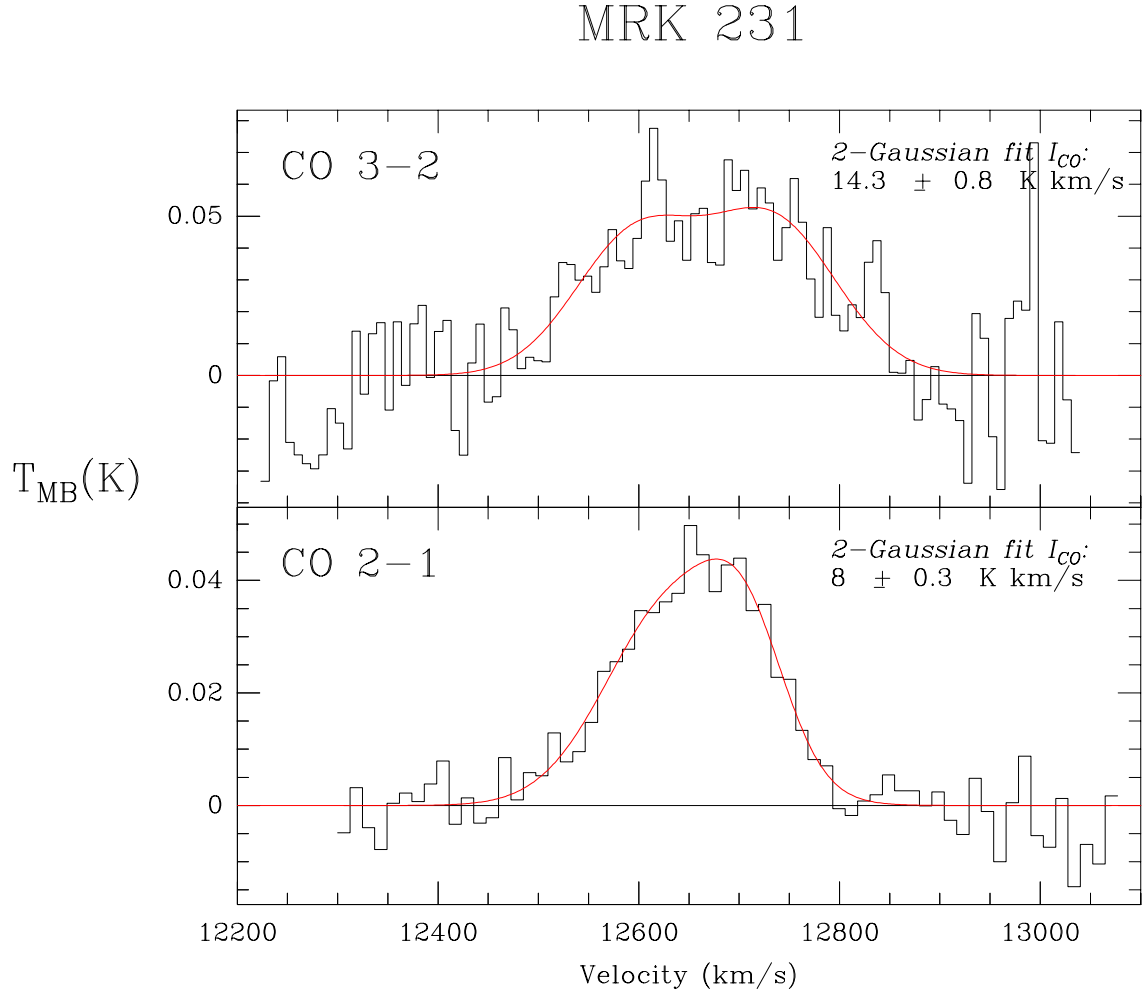


Fig. 7.— Mrk 273 in CO $3 \rightarrow 2$ and $2 \rightarrow 1$.

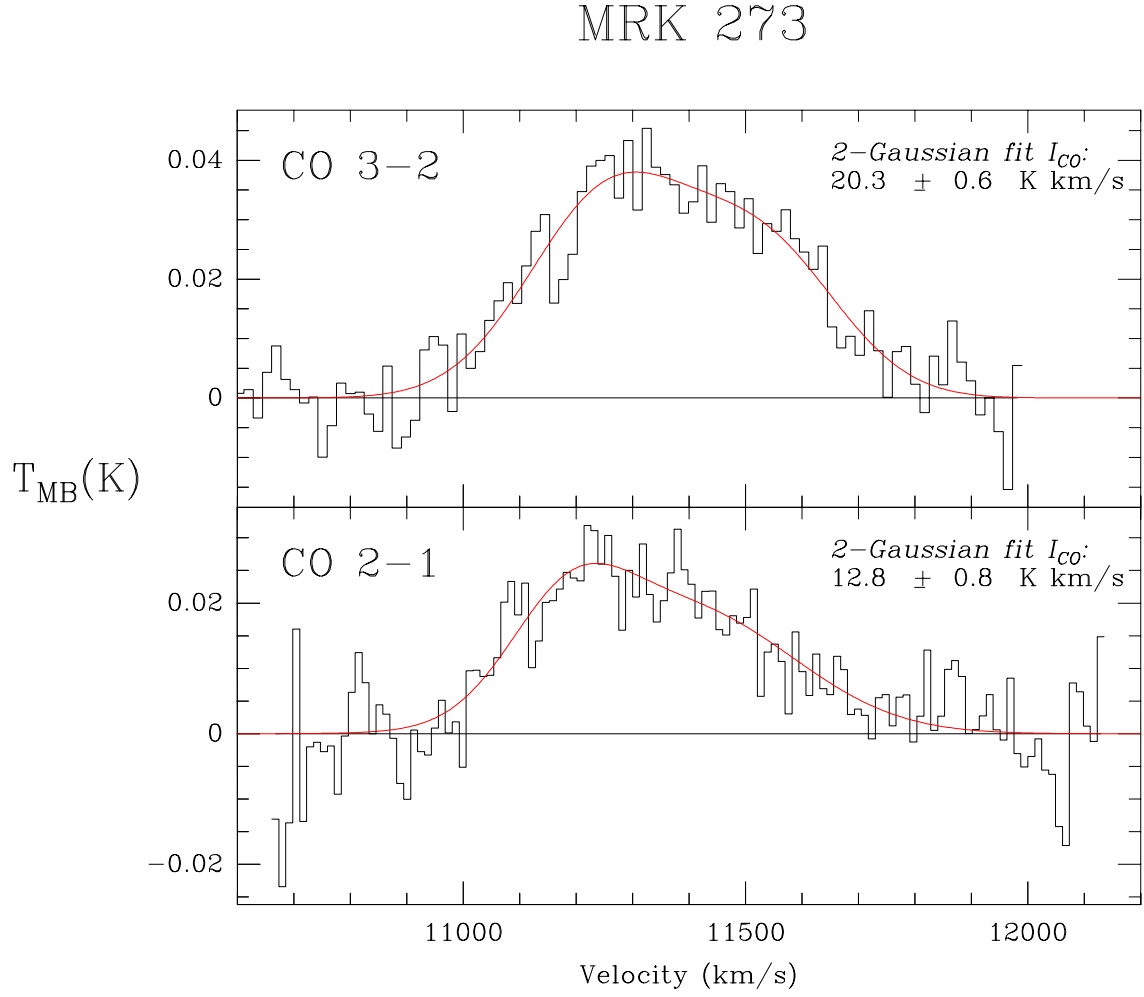


Fig. 8.— Arp 220 in CO $3 \rightarrow 2$ and $2 \rightarrow 1$.

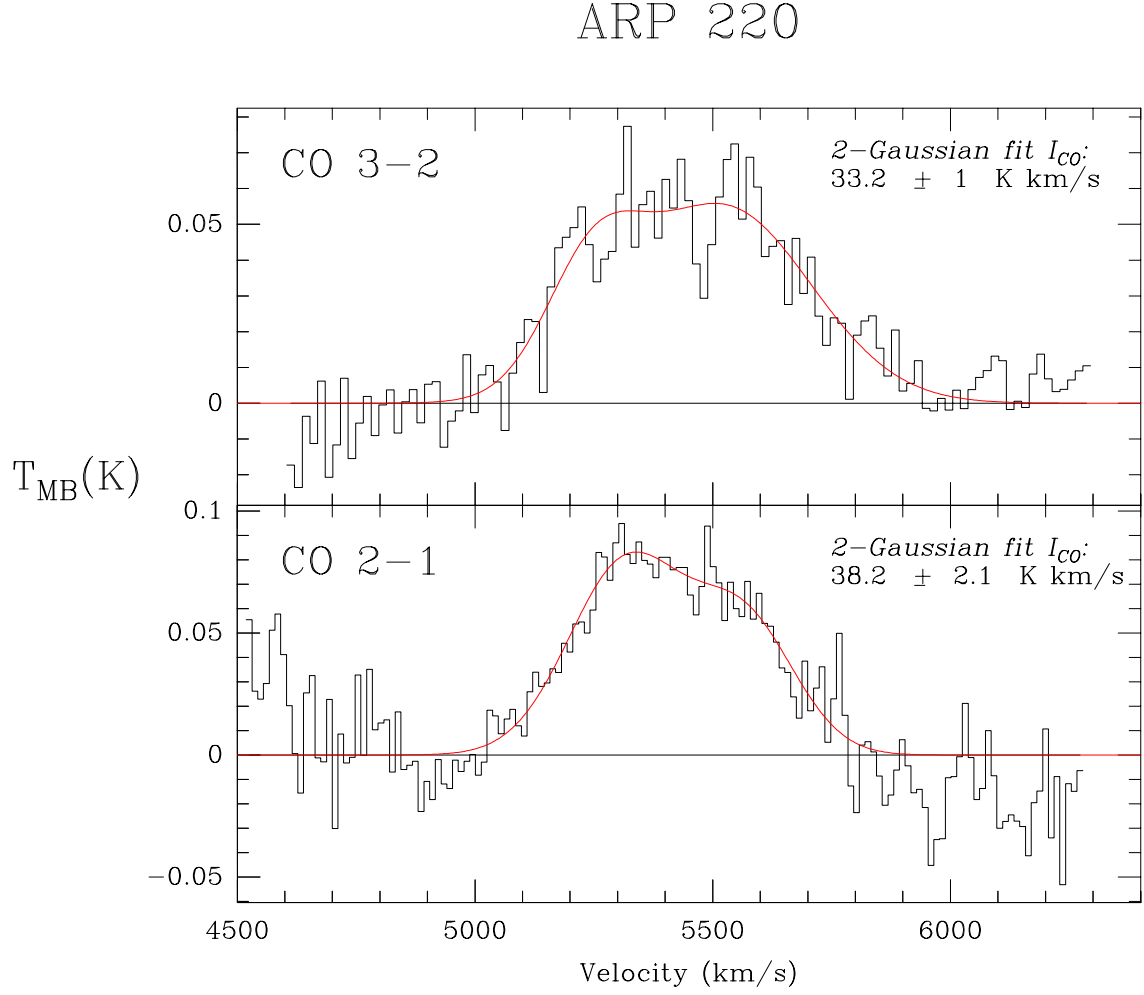


Fig. 9.— NGC 6090 in CO $3 \rightarrow 2$ and $2 \rightarrow 1$.

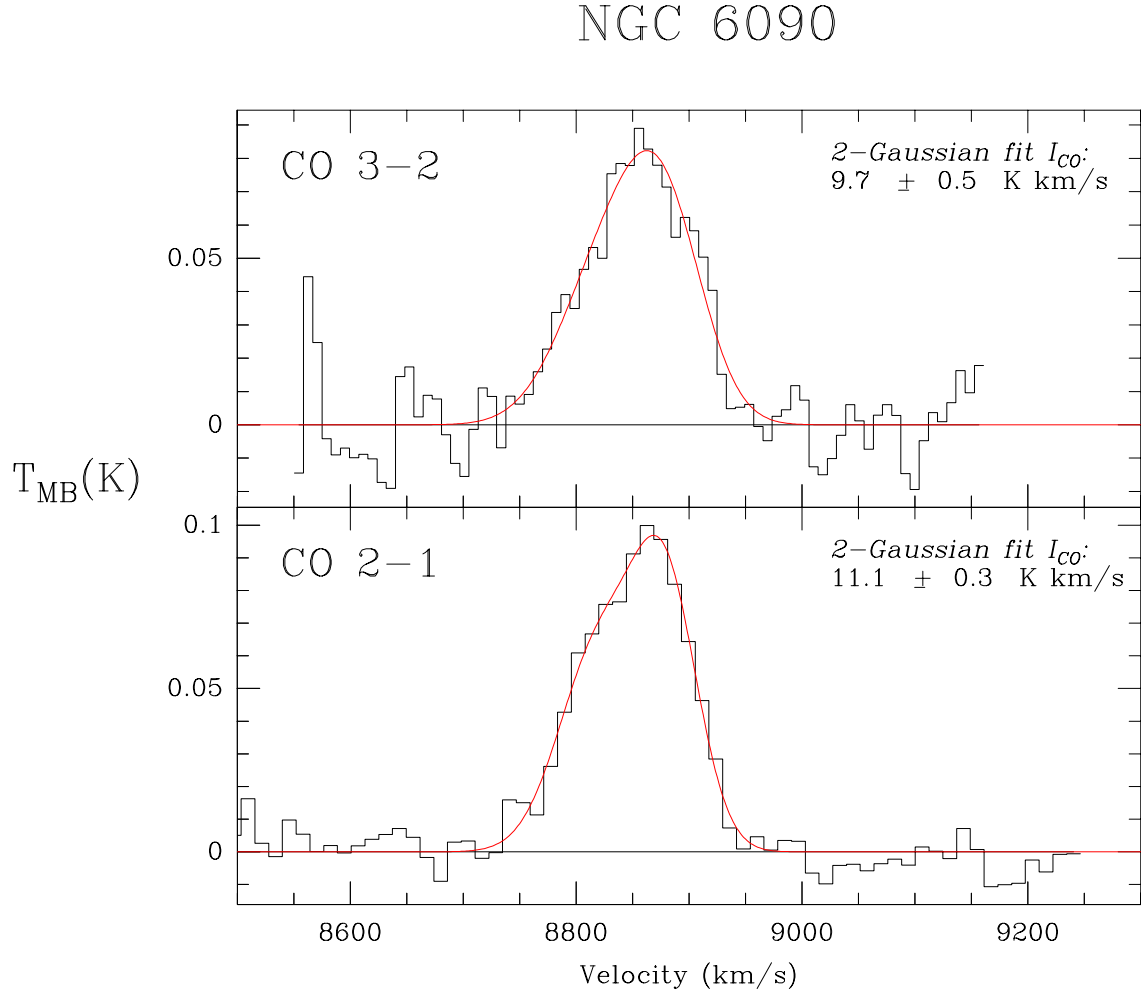


Fig. 10.— NGC 6090 in CO $6 \rightarrow 5$.

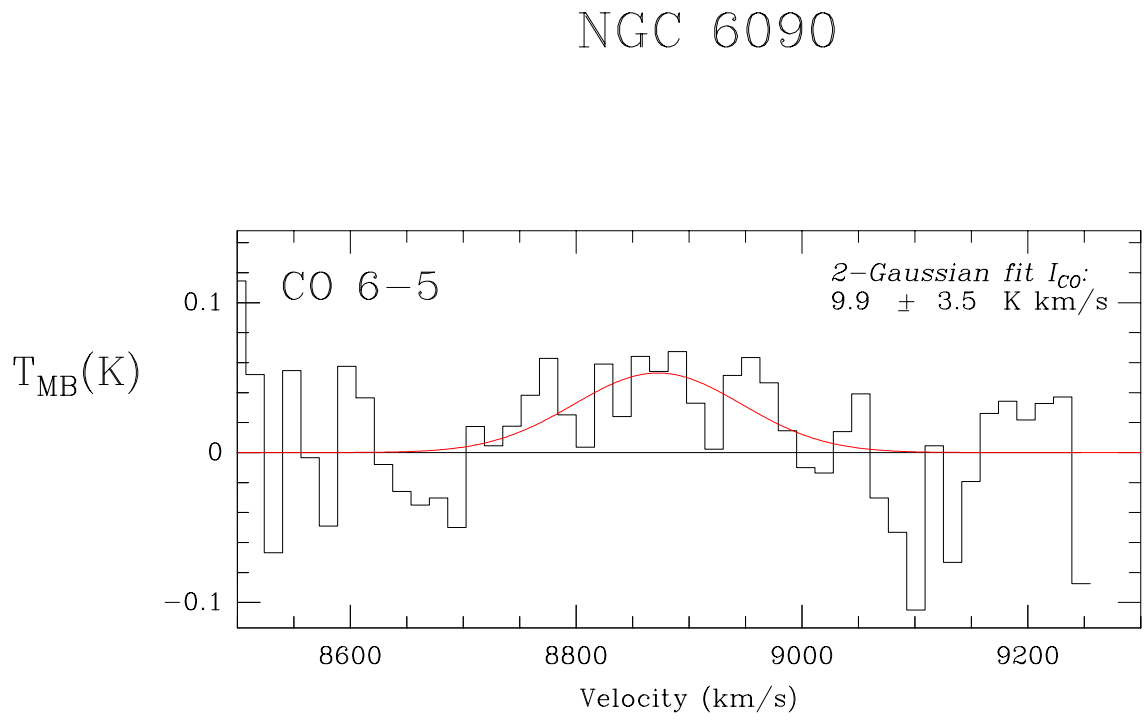


Fig. 11.— NGC 6240 in CO $3 \rightarrow 2$ and $2 \rightarrow 1$.

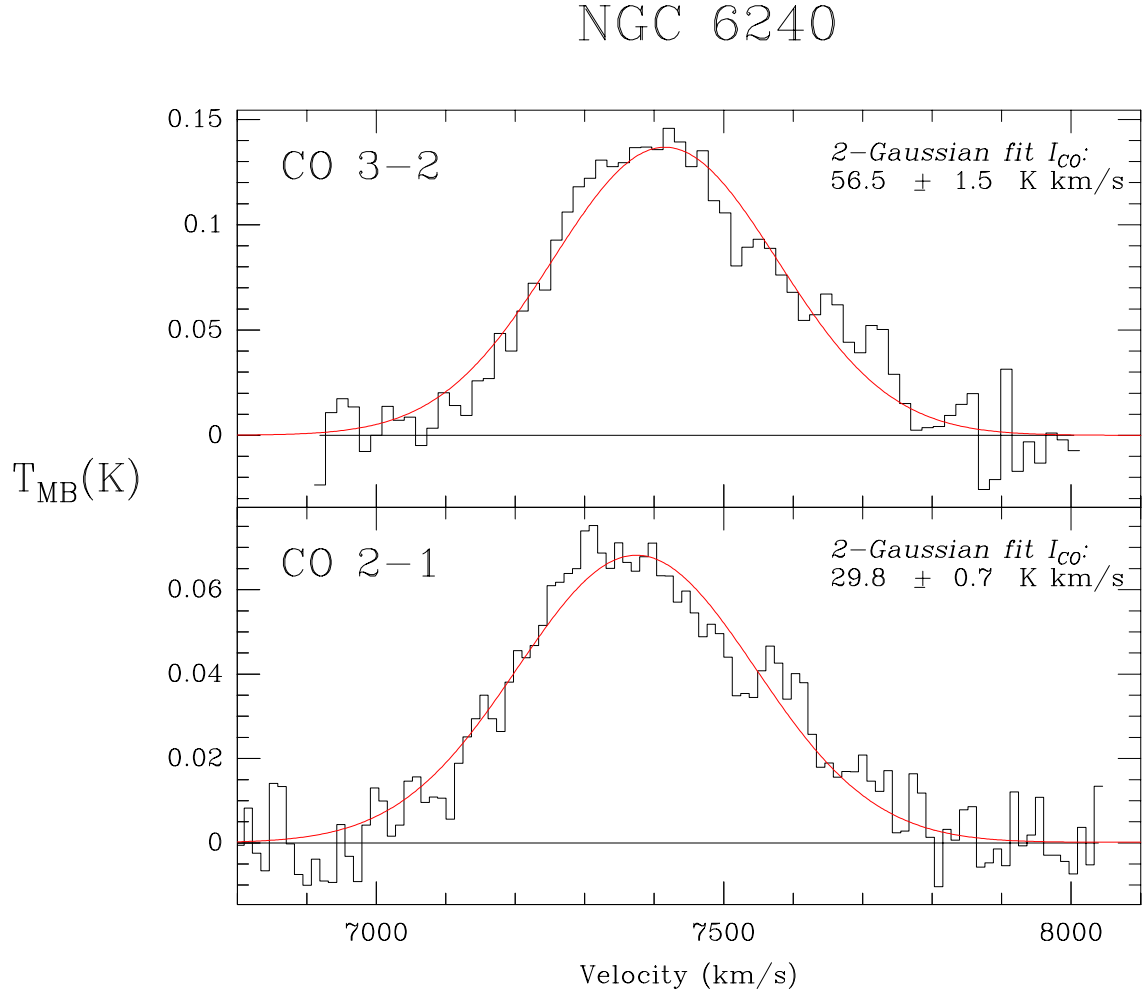


Table 1: CO $3 \rightarrow 2$ and $2 \rightarrow 1$ Observations of Luminous, Bright Infrared Galaxies

Galaxy	RA (1950)	Dec (1950)	CZ (km/s)	$T_{peak\,3 \rightarrow 2}$ (mK)	$T_{peak\,2 \rightarrow 1}$ (mK)	$I_{CO\,3 \rightarrow 2}$ (K km/s)	$I_{CO\,2 \rightarrow 1}$ (K km/s)	Flux Ratio $I_{3 \rightarrow 2}/I_{2 \rightarrow 1}$	Dilution-corrected Flux Ratio ¹
IR 0911	09:11:10.75	-10:07:04.2	16256	55	25	11.2 ± 0.4	4.4 ± 0.4	2.55 ± 0.25	1.13
NGC 3690	11:25:41.35	+58:50:16.5	3047	302	102	40.9 ± 2.0	16.7 ± 0.3	2.45 ± 0.13	1.09
Arp 299 A	11:25:44.20	+58:50:18.1	2747	200	230	46.8 ± 0.8	45.3 ± 0.7	1.03 ± 0.02	0.46
Mrk 231	12:54:05.00	+57:08:37.0	12139	48	42	16.2 ± 1.1	8.1 ± 0.3	2.00 ± 0.15	0.89
Mrk 273	13:42:51.70	+56:08:14.4	10906	37	17	20.2 ± 0.6	13.4 ± 0.8	1.51 ± 0.10	0.67
Arp 220	15:32:46.90	+23:40:07.7	5340	55	83	34.4 ± 1.0	38.0 ± 2.2	0.91 ± 0.06	0.40
NGC 6090	16:10:24.00	+52:35:11.0	8573	82	95	9.6 ± 0.5	11.0 ± 0.3	0.87 ± 0.05	0.39
NGC 6240	16:50:27.86	+02:28:58.9	7155	140	68	55.1 ± 1.5	28.0 ± 0.7	1.97 ± 0.07	0.88

¹ Beam Dilution Correction introduces a factor of

$$\left(\frac{\nu_{3 \rightarrow 2}}{\nu_{2 \rightarrow 1}} \right)^2$$

Table 2: Multitransition Observations

Galaxy	$I_{CO\,6 \rightarrow 5}$ (K km/s)	$I_{CO\,4 \rightarrow 3}$ (K km/s)	Flux Ratio $6 \rightarrow 5/2 \rightarrow 1$	Flux Ratio $4 \rightarrow 3/2 \rightarrow 1$	Flux Ratio $3 \rightarrow 2/2 \rightarrow 1$	Corrected Flux Ratio $6 \rightarrow 5/2 \rightarrow 1$	Corrected Flux Ratio $4 \rightarrow 3/2 \rightarrow 1$	Corrected Flux Ratio $3 \rightarrow 2/2 \rightarrow 1$
NGC 3690	16.9 ± 2.4	27.7 ± 6.1	1.01 ± 0.14	1.36 ± 0.30	2.45 ± 0.13	0.11	0.34	1.09
NGC 6090	11.9 ± 2.6		1.08 ± 0.24		0.87 ± 0.05	0.12		0.39